HHS Public Access

Author manuscript

Science. Author manuscript; available in PMC 2018 February 25.

Published in final edited form as:

Science. 2017 August 25; 357(6353): 811–815. doi:10.1126/science.aai7868.

Emergent Cellular Self-Organization and Mechanosensation Initiate Follicle Pattern in the Avian Skin

Amy E. Shyer[1,^,*], **Alan R. Rodrigues**[1,2,^], **Grant G. Schroeder**[1], **Elena Kassianidou**[3], **Sanjay Kumar**[3], and **Richard M. Harland**[1]

[1]Department of Molecular and Cell Biology, University of California, Berkeley, Berkeley, CA

[2]Department of Genetics, Harvard Medical School, Boston, MA

[3]Department of Bioengineering, University of California, Berkeley, Berkeley, CA

Abstract

The spacing of hair in mammals and feathers in birds is one of the most apparent morphological features of the skin. This pattern arises when uniform fields of progenitor cells diversify their molecular fate while adopting higher order structure. Using the nascent skin of the developing chicken embryo as a model system, we find that morphological and molecular symmetries are simultaneously broken by an emergent process of cellular self-organization. The key initiators of heterogeneity are dermal progenitors, which spontaneously aggregate through contractility-driven cellular pulling. Concurrently, this dermal cell aggregation triggers the mechanosensitive activation of β-catenin in adjacent epidermal cells, initiating the follicle gene expression program. Taken together, this mechanism provides a means of integrating mechanical and molecular perspectives of organ formation

---

During skin organogenesis, the structures that produce hair in mammals and feathers in birds, termed follicles, emerge in a spaced array. Prior to follicle formation in amniotes, the embryonic skin consists of a sheet of epithelial cells attached to a slab of mesenchymal cells via a basement membrane (Fig. 1A, B). Over the course of two days, this uniform tissue bilayer transitions into one studded with regularly spaced, multicellular aggregates, each with an activated follicle primordium gene expression program (Fig. 1A, B). Coordinating follicle spacing with appropriate gene expression changes is critical for the proper patterning of feathers in birds and hair in mammals. How this leap in complexity is reproducibly initiated remains unsolved (1,2).

---

*Correspondence should be addressed to: A.E.S. ashyer@berkeley.edu.
^These authors contributed equally to this work

Author Contributions:
A.E.S. and A.R.R. designed the experiments with additional contributions from G.G.S. A.E.S. and G.G.S. conducted the experiments. E.K. contributed the polyacrylamide gels, with technical and conceptual guidance from S.K. A.R.R. and A.E.S. wrote and prepared the manuscript with assistance from G.G.S., R.M.H., and S.K.

Supplementary Materials
Materials and Methods
Figs. S1 to S11.

Prior studies have posited that molecular patterns arise first and then dictate differential cell behaviors that cause changes in tissue structure (3, 4). This has led to the inference that follicle initiation is dependent on the establishment of a molecular prepattern. We began to question this model when we discovered that, in the avian skin, initial follicle fate markers, nuclear β-catenin (a master regulator of the follicle gene expression program, 5) and downstream expression of *bmp2* and *fgf10*, accompany rather than precede the earliest architectural changes of the follicle (Fig. 1B, fig. S1). At day 7 of development (E7), prior to the detection of these molecular markers, emerging follicles become detectable as stacked epithelial cells overlying aggregated mesenchyme (fig. S2). To confirm that initiation of structural changes does not rely on β-catenin activation, we promoted β-catenin degradation by culturing reconstituted skin explants prior to aggregation in XAV939, which stimulates β-catenin degradation (Supplementary Material, 6) (Fig. 1C). Although samples cultured in XAV939 lack nuclear β-catenin and *bmp2* expression, they are capable of forming spaced aggregates comparable to the follicle structure (Fig. 1C).

Given that follicle structures are capable of emerging in the absence of β-catenin activation, we investigated the driver of these structural changes. We were guided by the observation that as follicles emerge, the primordium basement membrane becomes increasingly arched, resembling a buckled sheet. Previous mechanical studies have shown that surface buckling can be caused by compression of a stiff film on an elastic substrate (7).

Given these observations, and more recent work highlighting the importance of a mechanical view (8, 9, 10), we began to explore a mechanism whereby follicle structure is initiated by compression. We first confirmed that such forces were sufficient to generate the architecture observed in follicles. To do so, we exploited the inherent tension present throughout the embryonic skin, which is evidenced by rapid shrinkage when a skin sample is excised (Fig. 2A, B). When the dorsal region of E6 skin is excised from the embryo and subjected to compression as tension is relieved, the entire tissue adopts an architectural profile akin to primordia, with bunched epithelial cells, aggregated mesenchyme, and a buckled membrane (Fig. 2C–E).

We next determined whether compression stems from cellular behaviors in the dermis or epidermis by separating these layers and monitoring basement membrane buckling as a marker of compression. Only the dermis forced the basement membrane to buckle and the epidermis to bunch, indicating that the dermal layer is the source of compression (Fig. 2F–I). We therefore hypothesized that the change in follicle structure is initiated by mechanical cross-talk whereby the dermal layer compresses the epidermal layer during follicle formation.

Having shown via tissue excision that ectopically generated dermal compression applied over the scale of minutes can simulate follicle morphology, we sought to articulate the native forces within the dermis that bring about follicle aggregation on the scale of hours. We ruled out forces generated from local proliferation because differential cell division does not occur prior to primordium formation (11). Instead, we focused on cellular rearrangement within the dermis as a potential mechanism of aggregation. Spontaneous mesenchymal cell aggregation has been observed *in vitro* when dissociated mesenchymal cells are cultured at

high density (1, 12, 13). The key drivers of such spaced aggregation have been formalized in several theoretical models (14, 15, 16, 17). Central to these models is cellular contractility within a rigid context. Mesenchymal cells have an intrinsic potential to aggregate, and as they do so, they amplify their potential to draw in additional cells. Thus, small, random fluctuations in cell density can be amplified to form larger aggregates as cells exert traction on each other. Second, this propensity for cellular aggregation must be resisted by surrounding material (with stiffness being a major component of resistance), which inhibits the formation of a single, large aggregate but permits a dispersed array.

We first tested for the necessity of an appropriately rigid context to promote the formation of spaced aggregates as well as the impact variation of stiffness could have on aggregate formation. We varied stiffness conditions using an *ex vivo* culture assay. When cultured atop a membrane in pilot experiments, spaced aggregates formed after 48 hours in culture (Fig. 3A, fig S3). However, when explants were cultured freely floating, they underwent extreme contraction and subsequently failed to form a pattern, underscoring the need for a stiff culture environment (fig. S3). To test if varying stiffness could modify aggregate pattern, we cultured skin explants on fibronectin-coated, polyacrylamide gels of progressive stiffness. Similar to freely floating explants, culture on soft gels allow the tissue to markedly contract with no clear emergence of aggregate pattern (Fig. 3A). Conversely, culture on the stiffest gel resulted in thin, stretched skin with either sparse or no pattern (Fig. 3A). At intermediate stiffness, however, explants formed aggregates where spacing between aggregates increases as a function of stiffness (Fig. 3A–D).

We then tested the necessity of cellular contractility for aggregate formation as well as the effect of varying contractility on pattern. Explants were cultured on a membrane or on collagen gels seeded with beads for detecting gel deformation. Tissues treated with high levels of blebbistatin, a myosin II inhibitor (18, 19), showed no increase in sub-adjacent gel bead density, indicating an effective pharmacological ablation of cellular contractility (fig. S4). This loss of contractility resulted in an abnormally large, thin tissue and an absence of any aggregate pattern (Fig. 3E). We also tested an independent inhibitor of myosin II activity, ROCK inhibitor Y27632, and observed similar disruption of pattern formation (fig. S5). In contrast, tissues treated with high levels of calyculin A, a myosin II activator (20), significantly increased sub-adjacent collagen gel bead density, indicating an effective pharmacological augmentation of cellular contractility (fig. S4). Increased contractility led to decreased tissue surface area and increased thickness, as well as the elimination of pattern (Fig. 3E). To rule out the possibility that the effects observed when myosin II activity was altered were through changes in cell division, we confirmed that proliferation was not altered by these drugs (fig. S6). Strikingly, between the extremes of traction, we find the sizing of primordia was progressively tuned (Fig. 3A). Even with a uniform starting area, the final number of primordia per sample increased at lower contractility and decreased at higher contractility, demonstrating that perturbing contractility does not result in the simple scaling of a bud prepattern (Fig. 3E–H).

These results are consistent with a model in which cellular contractility serves as a local activator and substrate stiffness serves as a long-range inhibitor of follicle aggregate formation. Thus, follicles emerge through a mechanical instability that spontaneously

generates an increase in morphological complexity. Of note, this mechanism bears resemblance to Alan Turing's models of chemical patterning, in which local activation competes against long-range inhibition (21). However, in this context, the key unit of pattern occurs at the cellular level and not the molecular.

Although this model of mesenchymal cell generation of mechanical instability provides an account of how follicle structure is initiated, it alone does not account for how changes in gene expression are triggered. We considered a mechanism whereby β-catenin in epithelial cells acts as a sensor of mechanical compression triggered by dermal cell aggregation. This putative mechanism is based on three reinforcing lines of evidence. First, it has been established that nuclear β-catenin in the epidermis is the earliest known regulator of primordium specific gene expression (5Noramly1999). Second, β-catenin has been shown to serve as a sensor and transducer of mechanical stimulus in invertebrate embryos and tumors (22, 23). Third, experiments presented above argue that the dermal layer focally compresses overlying epithelial cells through mechanical cross-talk, suggesting a direct mechanical trigger.

To show that β-catenin nuclear localization is dependent on dermal compression, we pharmacologically manipulated cellular contractility in cultured skin explants. Very high levels of contractility led to nuclear β-catenin across the entire epithelium, indicating that the entire bud adopted a follicle gene expression program (Fig. 4A). Conversely, under very low levels of contractility, no nuclear β-catenin was observed across the epidermis (Fig. 4A). At intermediate levels of traction, when primordia size is tuned, nuclear β-catenin adjusted in a lock-step manner with dermal aggregation (fig. S7). In parallel to changes in contractility, analogous nuclear β-catenin responses were observed when tissue mechanics were manipulated through substrate stiffness (fig. S8).

To determine the immediacy of β-catenin response to physical compression, we cultured excised skin freely-floating in media to allow for rapid contraction on the order of hours. In contracted tissues, nuclear β-catenin was observed in the epidermis after just two hours, suggesting a direct response at the post-transcriptional level (fig. S9). In control conditions, when explants were cultured attached to the body to prevent tissue contraction, no nuclear β-catenin was observed in the epithelium (fig. S9).

To further confirm the mechanical activation of β-catenin, we assayed for Y654 phosphorylation. Functionally, this Src kinase-dependent modification allows for β-catenin release from E-cadherin at the membrane and for subsequent translocation into the nucleus (24, 25). As predicted, Y654 staining was only observed in forming primordia (fig. S10). Tissue with ectopically high compression showed broad Y654 staining, while tissue with ablated compression showed none (fig. S10, S11). Y654 staining was also lost when tissues were cultured in the presence of SKI-1, an inhibitor of Src kinase activity, confirming the Src-dependent nature of this phosphorylation in the skin (fig. S11).

Finally, to confirm that this mechanical activation of β-catenin leads to activation of the downstream follicle gene expression program, we assayed expression of *bmp2*. Indeed, *bmp2* was also broadly expressed across the epidermis in highly contracted samples and no

bmp2 expression was seen in the uncompressed epidermis (Fig. 4B). This loss of expression was rescued through the addition of BIO to inhibit cytosolic degradation of β-catenin (fig. S10). Together, these results demonstrate that mechanically triggered movement of β-catenin to the nucleus is sufficient to initiate the primordia gene expression program.

Here we identify key initiators of follicle structure and fate in the skin. Our findings argue that the mechanics of cellular self-organization and structural rearrangement are critical not only for creating follicle shape but also for triggering the follicle gene expression program. Critically, tissue symmetry is broken mechanically and then directly conveyed to the genome via β-catenin mechanosensation. We propose that a similar mechanism could be at play in other contexts where tissue structure and fate decisions co-emerge in the absence of molecular pre-pattern.

Supplementary Material

Refer to Web version on PubMed Central for supplementary material.

Acknowledgments

We thank C. Miller and C. Exner for feedback on the manuscript, J. Tucher, H. Miller, and R. Parish for assistance with experiments, and G. Oster for his pioneering theories and thoughtful discussion. We gratefully acknowledge the support of the Miller Institute (A.E.S.), the HHMI International Student fellowship and Siebel Scholars Program (E.K), UC Berkeley SURF (G.G.S.), Endowed chair funds, C.H. Li Distinguished Professor funds, and NIH R01 GM42341 (R.M.H.) and NIH R21 EB016359 and R01 NS074831 (S.K.).

References

1. Harris AK, Stopak D, Warner P. J Embryol Exp Morphol. 1984; 80:1–20. [PubMed: 6747520]
2. Michon F, et al. Development. 2008; 135:2797–805. [PubMed: 18635609]
3. Noramly S, Morgan BA. Development. 1998; 125:3775–87. [PubMed: 9729486]
4. Widelitz RB, Chuong CM. J Investig Dermatol Symp Proc. 1999; 4:302–6.
5. Noramly S, Freeman A, Morgan BA. Development. 1999; 126:3509–21. [PubMed: 10409498]
6. Jiang TX, et al. Development. 1999; 126:4997–5009. [PubMed: 10529418]
7. Brau F, et al. Nature Physics. 2011; 7:56–60.
8. Howard J, Grill SW, Bois JS. Nature Reviews Molecular Cell Biology. 2011; 12:392–398. [PubMed: 21602907]
9. Munjal A, Philippe JM, Munro E, Lecuit T. Nature. 2015; 524:351–355. [PubMed: 26214737]
10. Shyer AE. Science. 2013; 342:212–8. [PubMed: 23989955]
11. Desbiens X, Turquez N, Vandenbunder B. Int. J. Dev. Biology. b. 1992:373–380.
12. da Rocha-Azevedo B, Grinnell F. Exp Cell Res. 2011; 319:2440–6.
13. da Rocha-Azevedo B, Ho CH, Grinnell F. Exp Cell Res. 2013; 319:546–55. [PubMed: 23117111]
14. Oster GF, Murray JD, Harris AK. J Embryol Exp Morphol. 1983; 78:83–125. [PubMed: 6663234]
15. Murray JD, Oster GF. IMA J Math Appl Med Biol. 1984; 1:51–75. [PubMed: 6600092]
16. Perelson AS, et al. J Math Biol. 1986; 24:525–41. [PubMed: 3805909]
17. Heisenberg CP, Bellaïche Y. Cell. 2013; 153:948–962. [PubMed: 23706734]
18. Beningo KA, et al. Arch Biochem Biophys. 2006; 456:224–31. [PubMed: 17094935]
19. Straight AF, et al. Science. 2003; 299:1743–7. [PubMed: 12637748]
20. Chartier L, et al. Cell Motil Cytoskeleton. 1991; 18:26–40. [PubMed: 1848484]
21. Turing AM. Philosophical Transactions of the Royal Society of London. Series B, Biological Sciences. 1952; 237:37–72.

22. Brunet T, et al. Nat Commun. 2013:4.
23. Fernandez-Sanchez ME, et al. Nature. 2015; 523:92–5. [PubMed: 25970250]
24. Lilien J, Balsamo J. Curr Opin Cell Biol. 2005; 17:459–65. [PubMed: 16099633]
25. van Veelen W, et al. Gut. 2011; 60:1204–12. [PubMed: 21307168]
26. Lee JP, Kassianidou E, MacDonald JI, et al. Biomaterials. 2016; 102:268–276. [PubMed: 27348850]

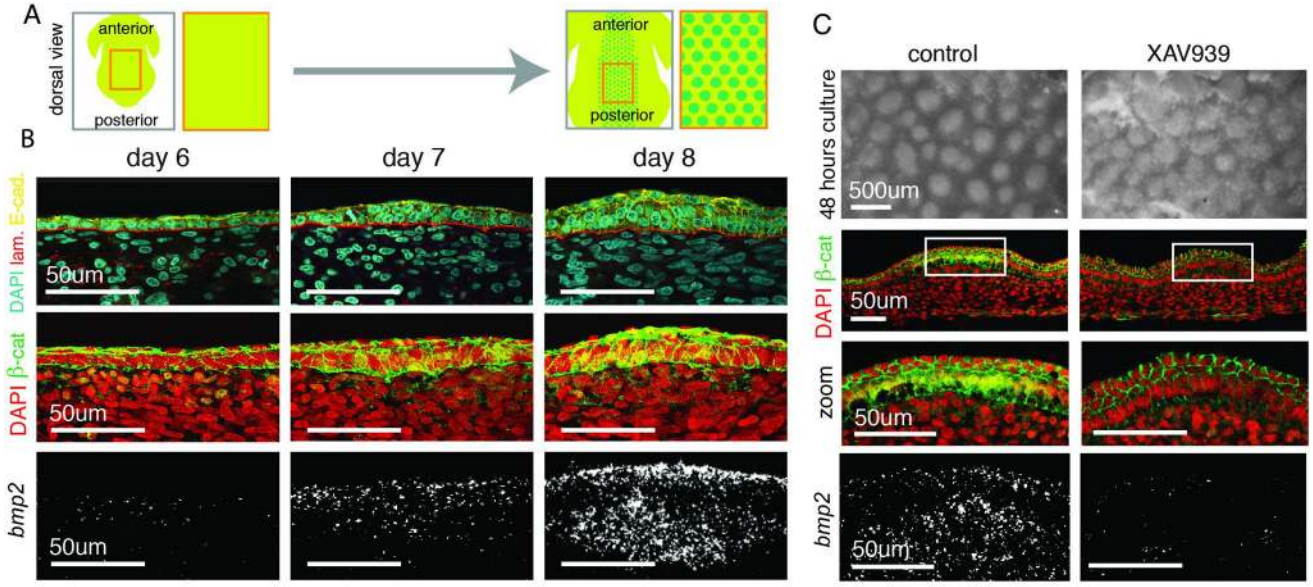

Figure 1. Feather primordium formation initiates with a co-aggregation of the epidermal and dermal cells

(A) An array of feather follicle primordia forms by E8. **(B) Top** - Cross-section of embryonic chicken skin antibody stained with DAPI, laminin (basement membrane), and E-cadherin (epidermal cell boundaries); Middlie - localization of β-catenin protein; Bottom - FISH for *bmp2* as a feather primordium forms from day 6 to day 8. **(C)** Reconstitution culture with or without XAV939: primordium structures initiate in the absence of nuclear β-catenin and localized *bmp2*. Lack of sharp boundaries in the XAV939 condition suggests a role for localized signals in refining primordia domains (n=3).

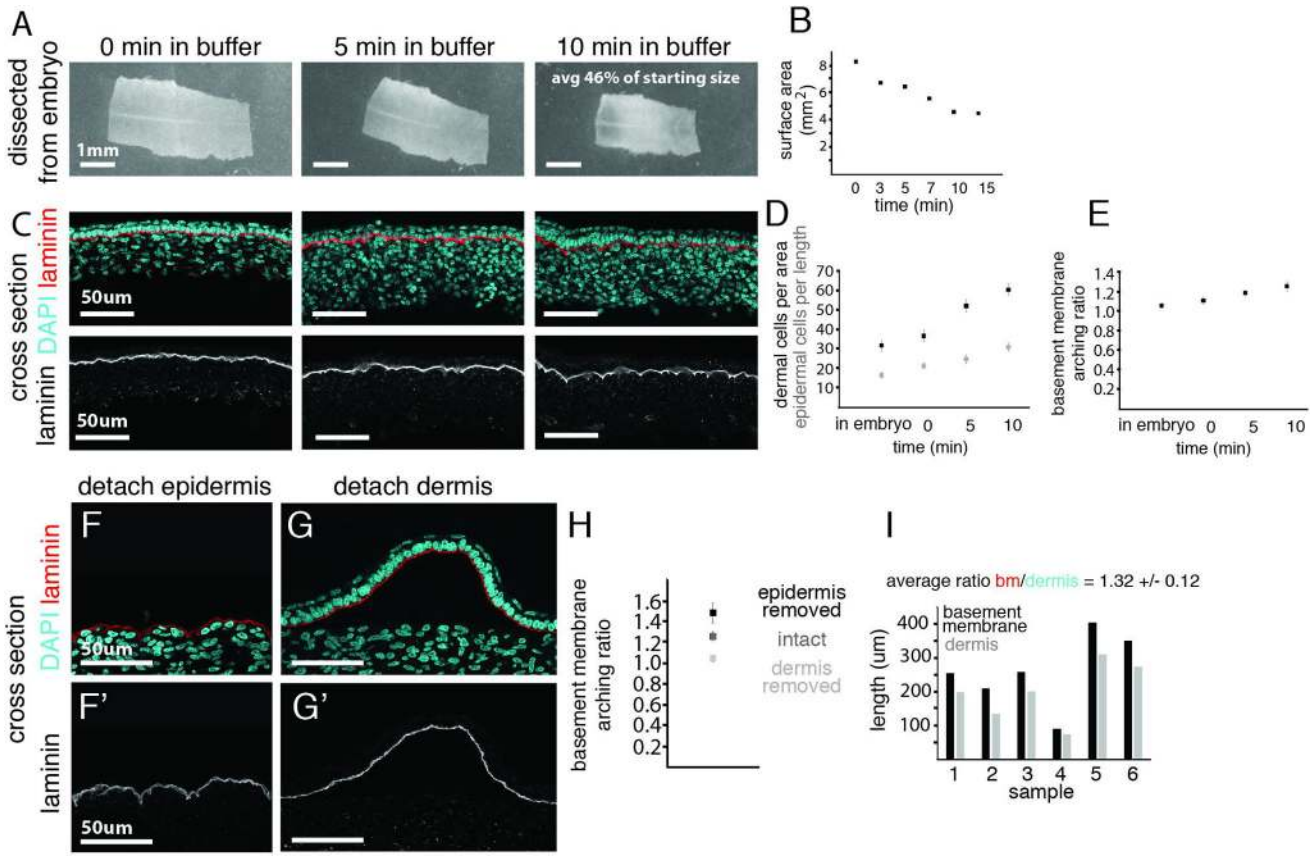

Figure 2. Primordium architecture arises upon ectopic compression, derived from dermal cell contraction

(A) E6 skin immediately after being dissected from the embryo, after 5 and 10 minutes in buffer; quantification of tissue area **(B)**. **(C)** Cross-section of the dissected skin sample over time with lower panels highlighting basement membrane shape. **(D)** Quantification of dermal cell density (cells per 50μm by 50μm) and epidermal cell density (cells per 100μm) over time in buffer. **(E)** Quantification of the basement membrane arching ratio (length per 100μm of the tissue). Effect on basement membrane architecture upon separation from epidermis **(F)** or dermis **(G)** - fixed after 10 minutes. Arching increases when the dermis remains attached, and decreases when the dermis is removed, quantified in **(H)**. **(I)** Comparison of separated lengths of the basement membrane and epidermis (black) to the length of the dermis (gray). Error bars are +/− SD (n>3 and at least three measurements per sample).

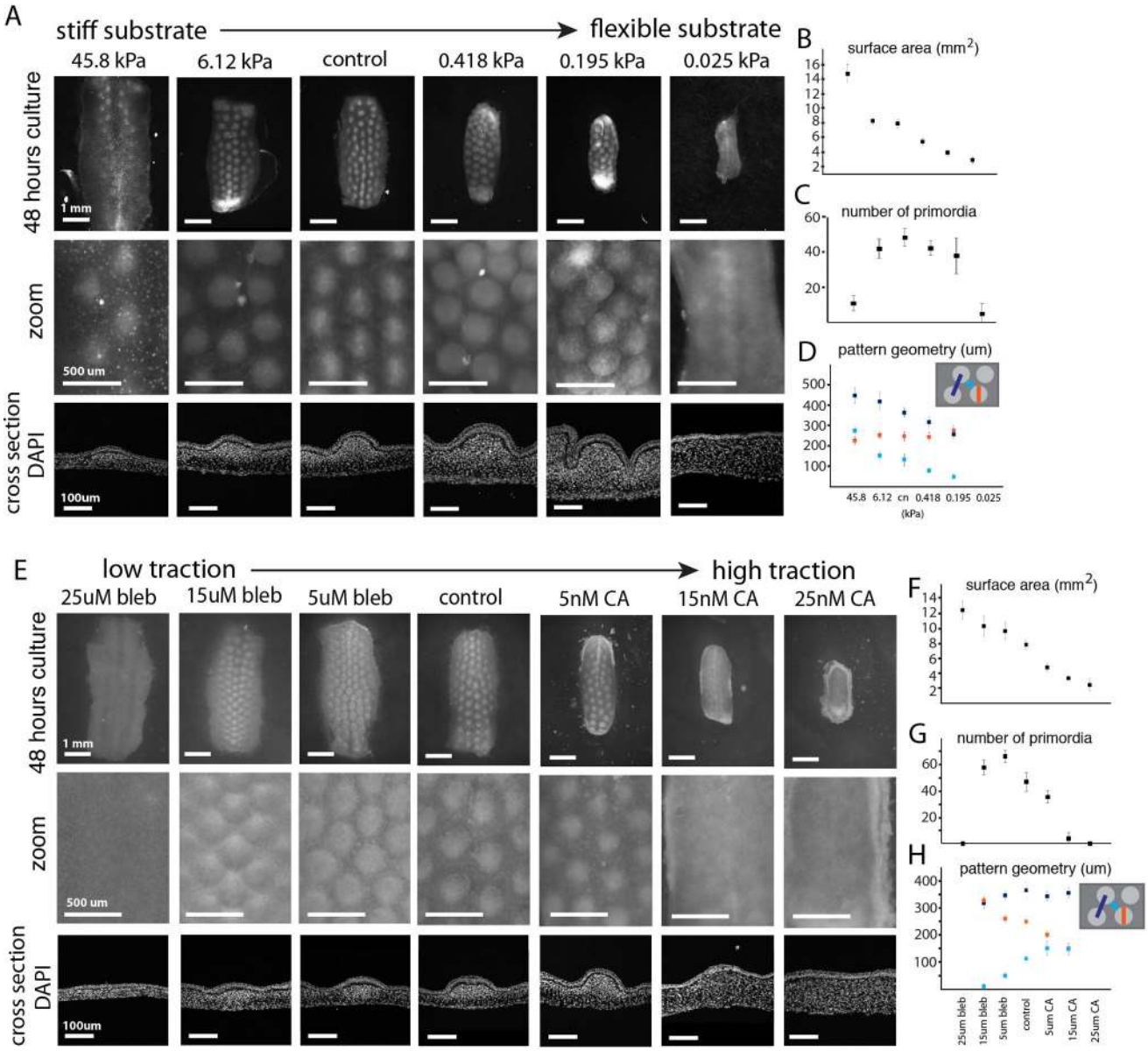

Figure 3. Cellular contractility within a rigid context leads to primordia emergence and pattern formation

Skin samples cultured on gels of high stiffness to low stiffness (values given are storage moduli) **(A)** and samples grown across a spectrum of contractility through pharmacological inhibition with blebbistatin or activation with calyculin A **(E)** as compared to control cultured on the filter membrane; higher magnification and cross sections below. Quantifications of surface area **(B, F)** and **(C, G)** number of buds per sample (n>3). **(D, H)** Quantification of pattern geometry across traction conditions (n>3, at least three measurements per sample). Error bars are +/− SD.

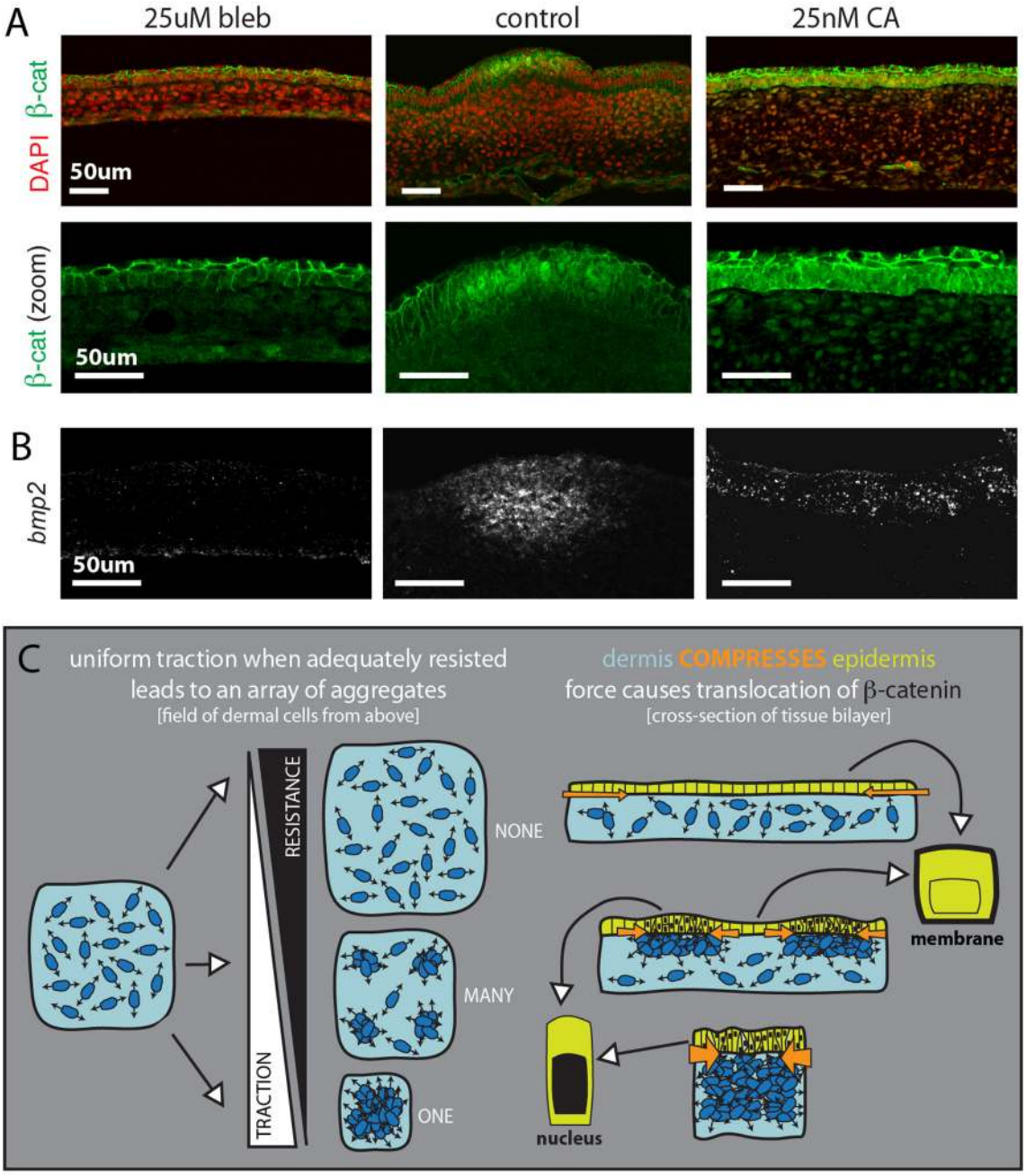

Figure 4. Movement of β-catenin to the nucleus in the forming primordium is mechanically triggered and upstream of the primordia gene expression program

(A) β-catenin localization and FISH for *bmp2* **(B)** in samples with low (left) and high (right) contractility as compared to the control sample (center) (n=3). **(C)** Model: A field of dense, contractile dermal cells will resolve into many spaced aggregates if cell contractility is met with resistance. If resistance is too too low (top) or too high (bottom), cells will be unable to pull into any aggregates or collapse into a single aggregate, respectively. Dermal cell aggregation compresses the adjacent epidermis focally, bunching the epidermal cells of each

primordium. Compression of the epidermis is sensed through the protein β-catenin, which responds to this force by moving to the nucleus.